



# A Novel Multi-Parameter Calibrator for Ventilator Tester Based on Reciprocating Plunger

X. Zheng, X. Zhipeng, J. Qing, Z. Gaoming, T. Jianbing

*Zhejiang Provincial Key Laboratory of Flow Measurement Technology, China Jiliang University, Hangzhou 310018, China  
E-mail (corresponding author): tangjb@cjlu.edu.cn*

---

## Abstract

Ventilators are widely needed when the COVID-19 is a global outbreak, and they are used to provide mechanical ventilation for patients who are physically unable to breathe, or breathe insufficiently. A ventilator tester is an instrument used to verify and calibrate ventilation parameters of ventilators like gas flow, tidal volume, frequency. As a measuring device, the ventilator tester also needs to be calibrated periodically. And different parameters are usually calibrated with different devices. In order to improve calibration efficiency and accuracy, a novel multi-parameter calibrator for ventilator tester based on reciprocating plunger is proposed in this work. The system composition is introduced and mathematical models are deduced. According to calibrating regulation, different calibrating modes are simulated and realized.

---

## 1. Introduction

As a device that can improve respiratory function and reduce the attrition of respiratory function, a ventilator is widely used in various medical institutions, emergency, ambulance, home care and other situations<sup>[1]</sup>. And since 2020, the new coronavirus COVID-19 has ravaged the world. Because the infected patients will suffer from pneumonia and cannot breathe naturally, they must use the ventilator to survive<sup>[2]</sup>.

Besides, a ventilator tester is a special measuring instrument used to verify and calibrate the mechanical ventilation metrology parameters of the ventilator. However, the internal sensor indicators will also deviate after a period of use, In order to ensure daily safe use and accurate measurement, it is also particularly important to carry out regular measurement and calibration on the ventilator tester.

The essence of the ventilator is to send gas to the patient at a certain flow and pressure, so that the patient can exchange gas. How to generate and accurately control the dynamic flow is the most basic and core technical link of the standard device of the ventilator tester. Although some research institutions have carried out study on standards, specifications and test devices for ventilator and respiratory simulation device, most researches focus on detecting the static flow, pressure and other parameters of ventilator tester. With the development of industrial technology, dynamic response performance of gas flowmeter is gradually required. Dynamic flow measurement performance has become one of the important indexes that can not be ignored in evaluating flow instruments<sup>[3]</sup>.

Reciprocating piston motion supported by servo control is one of the methods for dynamic flow generation. The thermostatic chamber unsteady gas flow generator developed by Japanese scholars Kawashima and Kagawa can produce sinusoidal oscillating flow with a frequency of 20Hz and an uncertainty of 5%<sup>[4]</sup>. And the unsteady gas flow generator developed by Tatsuya Funaki, which can be used to evaluate the dynamic characteristics of respiratory gas flowmeter, with an uncertainty of 4.8%<sup>[5-6]</sup>. Wang Tao from Beijing University of technology developed a gas dynamic flow generator with flow feedback, which can generate a flow above 0.2 kg/min with a frequency of 10Hz<sup>[7]</sup>. Zhang Enman et al. developed a set of square wave pulsating flow and error testing device<sup>[8]</sup>, and the square wave pulsating flow could be generated by reversing cylinder.

In addition, the Chinese Academy of Sciences has developed a set of calibration device for ventilator tester including oxygen concentration mixed detection module, static detection module and dynamic detection module. The dynamic detection module adopted the volume control mode and all the parameters were stable and controllable, which can be used as a standard signal generator<sup>[9]</sup>.

In this work, the dynamic and static gas flow, pressure, respiratory frequency, tidal volume and oxygen concentration of the ventilator tester were integrated for calibration test. Besides, the reciprocating plunger was used to realize the flow generation, so as to calibrate and trace the dynamic and static flow and pressure, and realize the expansion of the flow range and the improvement of accuracy. The research results obtained in this work can be directly applied to the testing service of instruments and equipment such as ventilator testers

and pulmonary function instruments in the metrology institute.

## 2. Scheme design

### 2.1 Principle

The physiological respiration of the human body is to exhale air to or inhale air from the atmosphere by changing the volume of the chest cavity through contraction and expansion, thereby changing the volume of air in the lungs [10]. Ventilation mode known as breathing mode is a method of respiratory support that can help the patient obtain the required volume and pressure curve. Ventilation is usually realized by mechanical structure, so it is also called mechanical ventilation [11]. Generally, the mechanical breathing of ventilators can be divided into four types including controlled breathing, mixed breathing, supporting breathing and spontaneous breathing. Physiological indicators of normal respiration can be seen in Table 1 [12].

The reciprocating piston device designed in this work uses a cylinder to simulate the lung, and the gas flow is realized by the reciprocating movement of the piston in the cylinder. When simulating exhalation, the piston moves downwards, and the air source provides the cylinder with air for breathing. When simulated inspiration, the piston moves upward to deliver air, so as to realize the calibration of the instrument under test. In both processes, the movement of the piston can be controlled by software, and the volume of gas in the cylinder can be changed to achieve controllability of the device [13].

**Table 1:** Basic parameters and requirements of respiration.

Parameter	Parameter Scope	Permission Error
Flow range	(0.5~180) L/min	$\pm 3\%$
Frequency	(1~80) Times/min	$\pm 3\%$
Tidal Volume	(0~2000) mL	$\pm 3\%$
Time Ratio	1:1.5~1:2	
Inspiratory Flow Oxygen Concentration	21%~100%	$\pm 2\%$

### 2.2 Hardware structure

As shown in Figure 1, the entire calibration device consists of the static/dynamic pressure and flow calibration module and the oxygen concentration calibration module. Reciprocating piston module is used to simulate the breathing curve and generate static and dynamic flow. Oxygen concentration calibration is to output uniform and stable standard mixed gas by mixing high-purity nitrogen and medical high-purity oxygen according to the set proportion.

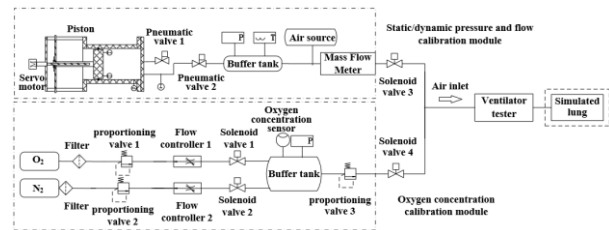


**Figure1:** Overall structure of the calibration device.

As shown in Figure 2, reciprocating piston device is composed of a servo motor, a coupling, a lead screw, a piston, a piston cylinder, temperature and pressure transmitter, a pneumatic valve, a buffer tank and a regulating valve. The servo motor connects the screw rod and the coupling to promote the movement of the plunger at the set speed, which can realize the gas exchange between the plunger cylinder and the atmosphere. The piston cylinder outlet is connected to the buffer tank, which can play a role in stabilizing the air flow. A mass flow meter is installed at the downstream to detect the output flow in real time.

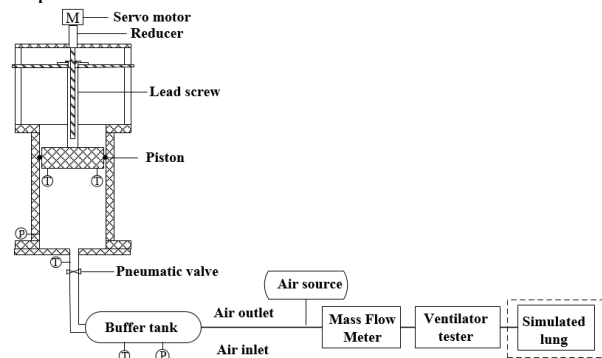


**Figure2:** Structure of the reciprocating piston device.

### 2.3 Control system and corresponding software design

The core control system is developed based on EtherCAT real-time Ethernet technology. All input and output signals can be transmitted to the upper computer (PC) or output to the specified port through IO module and coupler, and the servo driver can communicate, issue instructions and collect data [14].

Servo control adopts the technology of electronic CAM [15]. After processing the curve of electronic CAM and CAM table data, the upper computer can drive the servo motor to realize the piston variable speed motion according to the established trajectory parameters, and can return the motion parameters and motion state in real time.

The design structure of the control system is shown in Figure 3 below.

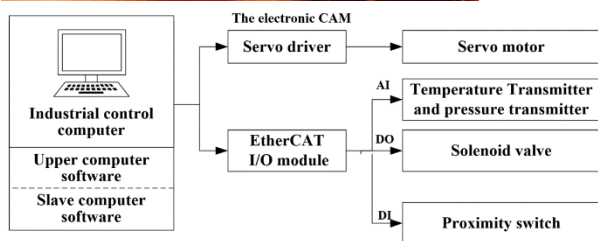


Figure3: Structure of the control system.

Both the upper computer software and the lower computer software are developed by TwinCAT. TwinCAT integrates real-time core, I/O data acquisition, sequence control (PLC), motion control (soft movement control), communication (ADS) and supporting tool software, which is very convenient for development and application.

The software of the lower computer mainly uses two parts of TwinCAT System Manager (TwinCAT System Manager) and PLC controller (TwinCAT PLC Control) [16]. TwinCAT system manager is the core configuration tool of the TwinCAT system, which manages the software task input and output and the physical input and output of the fieldbus connection,

TwinCAT PLC Control is a compilation environment for PLC logic and motion control. The motion control function of the axis: including the uniform motion of the axis, the absolute position motion, the relative displacement motion, the pause of the axis, the enable of the axis, the reset of the axis, etc. Mainly through integration in the system or library file can be called all kinds of motion control function blocks in PLC control compilation.

The electronic CAM is realized jointly by TwinCAT System Manager and TwinCAT PLC Control platform. Firstly, the track curve between the spindle (Master) and the Slave (Slave) similar to the mechanical CAM function is planned in the System Manager interface, so as to realize the control of one master axis to one or more slave axes. The motion relationship between the master and slave axes of the electronic CAM will move synchronously according to the designed and planned curve, and at the same time feedback the position information of the servo motor in real time, and control the follower to realize the motion similar to the motion law of the mechanical CAM.

PLC Control is responsible for starting, enabling, running and stopping of the master and slave axes, as well as the call of the CAM table, and the coupling and decoupling of the CAM. The electronic CAM implementation process is shown in Figure 4.

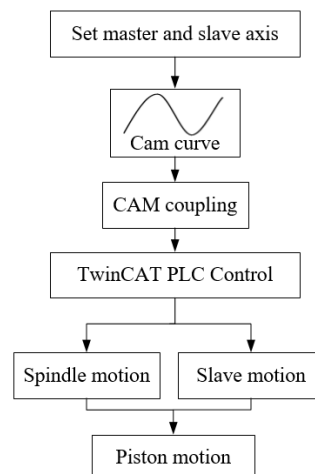


Figure 4: The electronic cam implementation process.

### 3. Theoretical model

#### 3.1 Theoretical model of ventilator-controlled ventilation mode

Controlled ventilation can be divided into volume controlled ventilation (VCV) and pressure controlled ventilation (PCV) [17]. In the VCV mode, the parameters such as the tidal volume, respiratory rate and respiratory ratio are controlled by the ventilator [18]. As shown in Figure 5, the flow rate waveform is square waves and the inspiratory flow rate is constant. The single breath cycle time is designed to be 3 s, and the maximum tidal volume is reached at 1.2 s. In the PCV mode, we set the airway pressure and frequency, and use deceleration flow to maintain the airway pressure at the pre-set level. As shown in Figure 6, the flow rate waveform is of decreasing wave and the inspiratory flow rate is decreasing [18]. The single breath cycle time is 3 s, and the maximum tidal volume reaches 1000mL at 1.5 s.

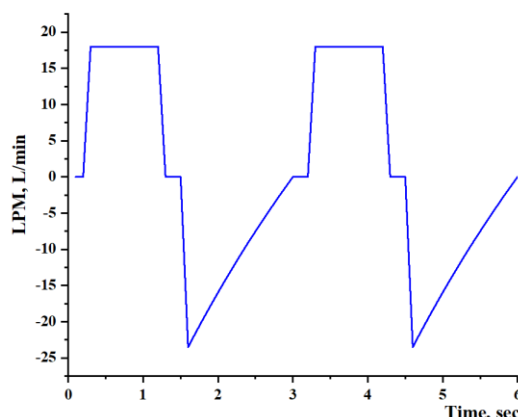


Figure 5: Variation in flow rate with time in the VCV mode.

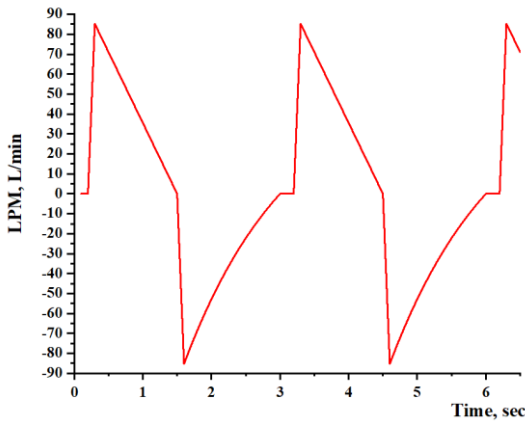


Figure 6: Variation in flow rate with time in the PSV mode.

### 3.2 Theoretical model of human respiratory curve

The respiratory curve of human body can be approximated to higher order cosine function<sup>[19]</sup>, on the base of which a model describing variation in flowrate with time for human body in the calm breathing state is established. As shown in Figure 7, the human respiratory cycle in the calm state is set to be about 3.20 s, and the maximum volumetric flowrate in the inspiratory and expiratory phases are about 42 L/min and 28.734 L/min respectively. The maximum tidal volume reaches 579 mL at about 1.30 s.<sup>[21]</sup> Besides, accumulating flowrates in the expiratory and inspiratory phases are equal.

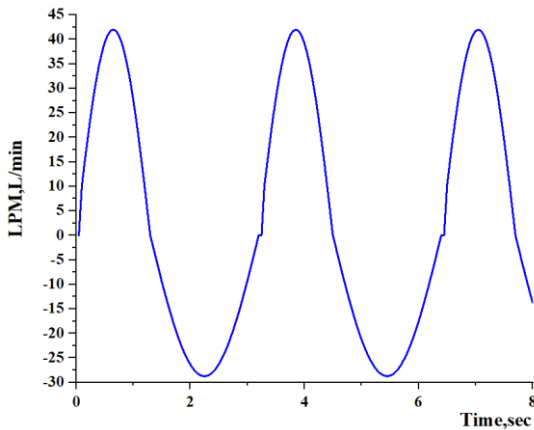


Figure7: Variation in respiratory flowrate with time in the calm state.

### 3.3 Static flow theory model

For the calibration of static flow, the constant flow rate curve is input to output standard flowrate. The static flow curve with a flowrate of 30 L/min is simulated, as shown in Figure 8.

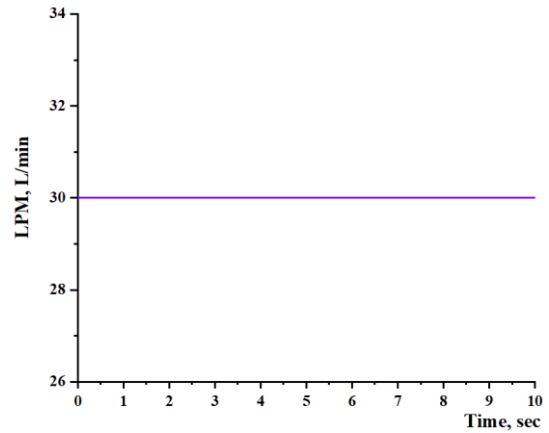


Figure 8: Static flow model curve.

### 3.4 Mathematical model of reciprocating plunger device

When the simulated exhalation plunger moves upward, the air source can provide the air for breathing to the cylinder, and the gas is exhausted from the inner diameter of the plunger cylinder through the pipe and the buffer tank. The mass flow rate of the gas exhausted can be calculated from the equation (1).

$$q_m = V\rho = \frac{\pi d^2 L\rho}{4t} \quad (1)$$

where  $q_m$  is the mass flow rate generated by the prover.  $L$  is the displacement of the plunger during operation.  $d$  is the diameter of the plunger.  $\rho$  is the gas density in the cylinder.  $t$  is the duration of piston's motion.

The ideal gas state equation is shown in Equation (2):

$$PV = nRT \quad (2)$$

where  $P$  is the pressure of the ideal gas,  $V$  is the volume of the ideal gas,  $n$  is the amount of substance of the ideal gas,  $R$  is the general gas constant,  $T$  is the temperature of the ideal gas. And the density expression of the ideal gas state equation is:

$$\rho = \frac{PM}{TRZ} \quad (3)$$

where  $M$  is the quantity of the ideal gas substance,  $Z$  is the gas compression factor.

In combination with equations (1) and (3), the relationship between piston speed and mass flow can be obtained:

$$q_{mt} = \frac{\pi d^2 P_t M}{4T_t R Z_t} v_t \quad (4)$$



where  $v_t$  is the operating speed of the piston at time ( $t$ ) under actual operating conditions [21].

#### 4. Simulation study

##### 4.1 Simulation system construction

Since the piston system is a dynamic system, its volume, temperature, pressure and heat transfer will change with the movement of the piston, and the gas itself has strong compressibility, the actual gas is more nonlinear. Therefore, the correspondence between the dynamic gas flow output and the piston speed cannot be obtained through theoretical analysis and calculation. In this paper, AMESim software simulation method is used to solve this problem.

And before establishing the simulation model, the following assumptions are made:

- (1) The temperature field and pressure field of the gas in the container are uniform;
- (2) When the gas flows through the orifice, it is a one-dimensional isentropic flow;
- (3) The gas viscosity is small, and the influence of the viscous resistance at the control section is not considered;
- (4) The gas density is small, and the influence of the gravitational field on the airflow is ignored.

Pistons and piston cylinders (piston components) can be found in the pneumatic component design library. Because the motor is driven by the screw as the input of the piston movement, the power of the plunger and the servo motor connected to the screw are simplified into the speed and displacement of the piston cylinder, which are realized through the input signal and the speed-displacement converter. The plunger is only driven by the bottom, and a zero-force source is connected to the pneumatic plunger element to provide the force of the plunger in the simulation model.

The outlet pipeline of the plunger cylinder and the buffer tank are simplified as a whole through a fixed container. The closed-loop control is introduced into the simulation model, the outlet pipeline is connected to the mass flow sensor as the feedback signal, and the PID controller is added. The overall simulation model of the closed-loop control of the dynamic gas flow generator is obtained, as shown in Figure 9.

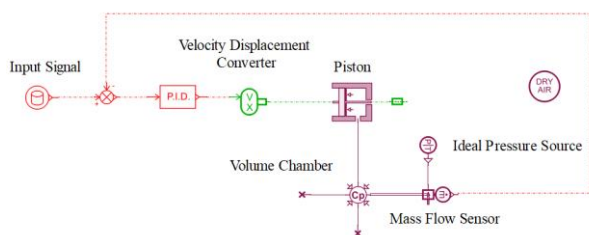


**Figure 9:** Closed-loop control simulation model of dynamic gas flow generator.

After the simulation model of the device is built, the parameters of components or sub-models in the model should be set before simulation. The specific parameters are shown in Table 2.

**Table 2:** Simulation basic parameters.

Parameter	Specific value
Piston diameter/ mm	400
Temperature/ K	299.15
Pressure/ hPa	1000.05

##### 4.2 Simulation curve processing

In order to facilitate the simulation and comparison with the experimental data of the mass flow meter, the gas flow unit L/min input into the simulation curve is now converted into g/s. Besides, the gas density can be derived from the formula according to the gas state equation [20].

$$\rho = \frac{P}{T} \cdot \frac{T_N}{P_N} \cdot \rho_N \quad (5)$$

where  $P$  represents the absolute static air pressure;  $T$  is the thermodynamic temperature of the air;  $P_N$  represents the absolute static pressure of the air under standard conditions, usually taking the value of 101325 Pa;  $T_N$  is the air thermodynamic temperature under standard condition, usually taking the value of 293.15K;  $\rho_N$  is the density of dry air under standard conditions, usually taking the value of 1.204 kg/m<sup>3</sup>.

According to the local temperature and pressure in Hangzhou in June, the absolute static pressure of the air is 1.0005×10<sup>5</sup>Pa, and the thermodynamic temperature of the air is 299.15K. The above data is brought into the formula to solve, and the air density is about 1.167334 kg/m<sup>3</sup>.

#### 5. Simulation results

In experiment, the flow curve and static flow curves of VCV, PCV and calm breathing are simulated under different tidal volume, and AMESim simulation is used to obtain CAM trajectories for corresponding motor experiments.

##### 5.1 Experimental results of the VCV mode

According to the VCV theoretical model curve in Figure 5, the maximum value of the tidal volume is set to 500mL at about 1.2 s when the breathing cycle is 3s, and the simulation experiment is performed. After the simulation signal is input, and the appropriate PID parameters are adjusted to make the mass flow curve basically consistent with the input simulation curve.

The required electronic CAM curve is obtained through simulation and compared with the actual motor running



trajectory. The displacement and velocity of the piston are shown in Figures 10 and 11 respectively.

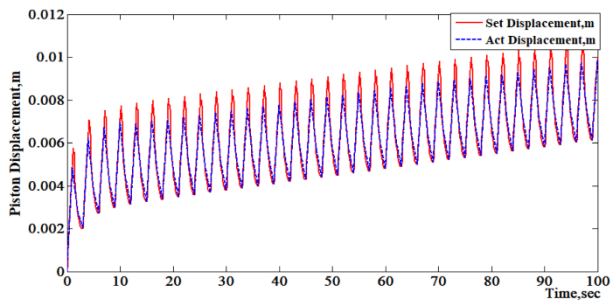


Figure 10: Piston displacement results in VCV.

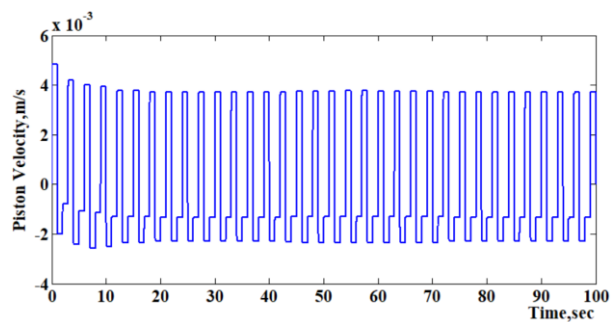


Figure 11: Piston velocity results in VCV.

### 5.2 Experimental results of the PCV mode

Similarly, in the PCV respiratory pattern, the maximum value of the tidal volume is set to 800mL at about 1.5 s when the breathing cycle is 3s. The experimental results are shown in Figures 12 and 13.

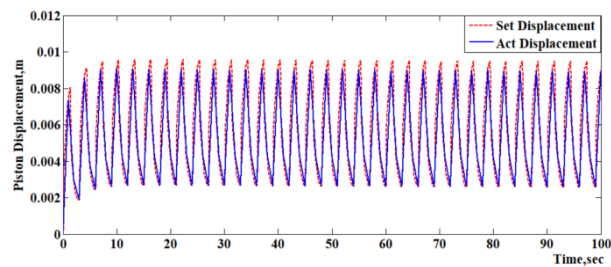


Figure 12: Piston displacement in PCV.

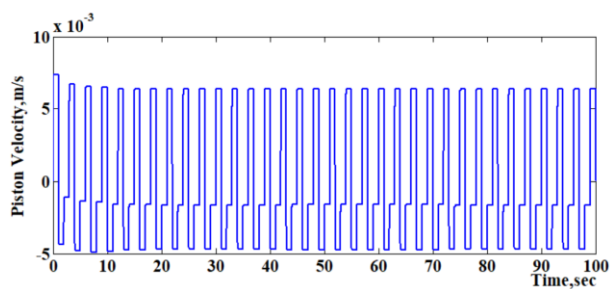


Figure 13: Piston velocity in PCV.

### 5.3 Experimental results of the calm breathing sate

FLOMEKO 2022, Chongqing, China

The single breathing cycle of the calm breathing mode is set to 3.2 s, and the maximum value of the tidal volume is set to about 579.3mL at 1.3 seconds. The results are shown in Figures 14 and 15.

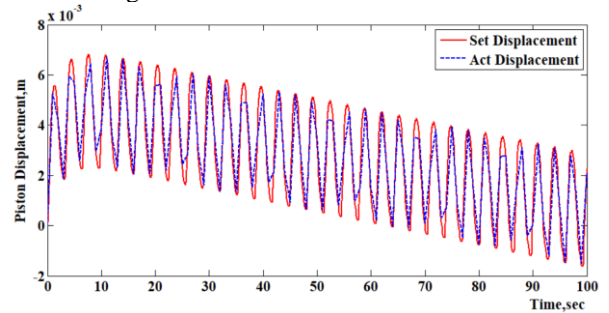


Figure 14: Piston displacement in calm breathing mode.

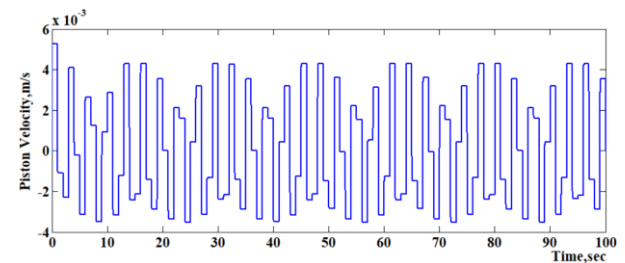


Figure 15: Piston velocity in calm breathing mode.

Through the simulation experiments of AMESim, it can be found that the output form of the flow rate and the speed of the piston do not correspond linearly, which is due to the compressibility of the gas, making the gas piston system a complex system of volume, temperature, pressure, and heat exchange area.

### 5.4 Experimental results of static flow

For the experiment of static flow, the constant flow rate of 30 L/min is simulated, and the results are shown in Figures 16 and 17.

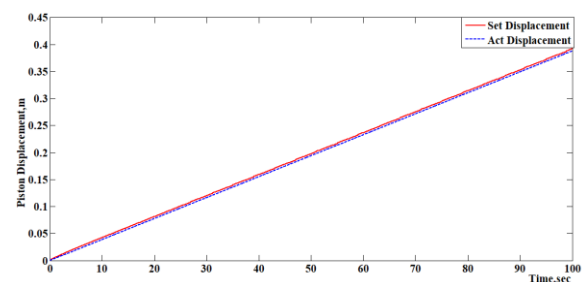


Figure 16: Piston displacement in static flow mode.

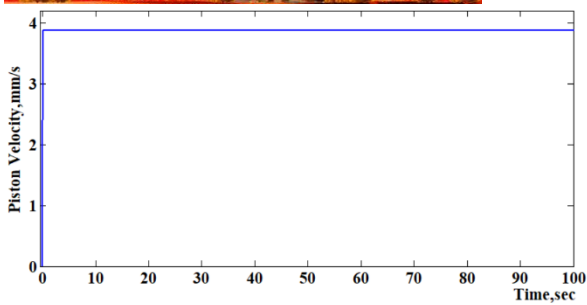


Figure 17: Piston velocity in static flow mode.

From the above experimental results, it can be found that there is some error between the input electronic CAM curve and the actual motor, especially at the peak. The main reason is that the physical limitations of the acceleration of the servo motor make it impossible to simulate the step of the flow or trajectory extremely accurately. Meanwhile, the control system of the whole device is open-loop, no real-time feedback, and the deviation of the flow or trajectory cannot be adjusted in time.

## 6. Conclusion

In this paper, a reciprocating dynamic gas flow generator is designed, and a system simulation model is built based on the AMESim simulation environment. Taking the dynamic gas flow of different breathing modes as the target, the required plunger running speed and trajectory curve are obtained. Meanwhile, the real-time controller based on TwinCAT is imported to realize a relatively smooth dynamic flow output. The experiments show that the method of deriving the trajectory curve through theoretical simulation to achieve dynamic flow output is feasible, but due to the limited time and conditions, the device needs to be further studied.

## References

- [1] Ki A, Sb B, Rv C, et al. Challenges and solutions in meeting up the urgent requirement of ventilators for COVID-19 patients - ScienceDirect[J]. *Diabetes & Metabolic Syndrome: Clinical Research & Reviews*, 2020, 14(4): 499-501.
- [2] Ali Ahmad Malik, Tariq Masood, Rehana Kousar, Reconfiguring and ramping-up ventilator production in the face of COVID-19: Can robots help? *Journal of Manufacturing Systems*, Volume 60, 2021, Pages 864-875.
- [3] Ye H C. Research on the Gas Dynamic Flow Test System. Zhejiang University, 2013.
- [4] KAWASHIMA K, KAGAWA T. Unsteady Flow Generator for Gases Using an Isothermal Chamber[J]. *Measurement*, 2003, 33(4) : 333-340.
- [5] T. Funaki, Study on flow rate control system of oscillatory gas flow generator[C], Proceedings of SICE Annual Conference 2010, 2010, pp. 1676-1681.
- [6] T. Funaki, Development of Unsteady Gas Flow Generator for Evaluating the Dynamic Characteristic of Respiratory Gaseous Flow Meter[J]. American Society of Mechanical Engineers, Fluids Engineering Division (Publication) FEDSM, v2, p185-192, 2010.
- [7] WANG T, WANG X X, PENG G Z. Design of Gas Unsteady Flow Rate Generator with Flow Feedback[C]. The 11th Youth Academic Conference of China Instrument and Control Society. Beijing: 《Chinese Journal of Scientific Instrument》, 2009: 195-198.
- [8] ZHANG N M, JIANG H C, SHEN W X. Study on Gas Pulsating Flow and Testing Device Technology[J]. *Metrology Science and Technology*, 2017(06): 16-18.
- [9] Chinese Academy of Metrology, Ventilator Tester Calibration Device, China, CN201410554972.5. 2014-12-24.
- [10] Warliah L, Rohman A S, Rusmin P H. Model Development of Air Volume and Breathing Frequency In Human Respiratory System Simulation[J]. *Procedia-Social and Behavioral Sciences*, 2012, 67:260-268.
- [11] Yuh-Chin T. Huang, Jaspal Singh. CHAPTER 22-Basic Modes of Mechanical Ventilation[M]. *Mechanical Ventilation*, 2008, 247-255.
- [12] JIF 1234-2018: Calibration Specification for Ventilators, 2018.
- [13] Dong F Y, Sun Q L, Guo L, Chen Z Q. Design and Implementation of a Simulated Lung System Based on PLC. *Automation & Instrumentation*, 2018, 33(3): 9-13.
- [14] Zhou J. Research on Collaborative Control of Double-Piston Gas Prover Based on EtherCAT. China Jiliang University, 2017.
- [15] Chang Y H, Chieng W H, Liao C S, et al. A novel master switching method for electronic cam control with special reference to multi-axis coordinated trajectory following[J]. *Control Engineering Practice*, 2006, 14(2):107-120.
- [16] Pang D F, Du H Q, Cui J. Design of Experimental Platform for Electromechanical Transmission Control Based on TwinCAT. *Science and Technology & Innovation*, 2020(18):130-131.
- [17] A.J. Garnero, H. Abbona, F. Gordo-Vidal, C. Hermosa-Gelbard, Pressure versus volume controlled modes in invasive mechanical ventilation, *Medicina Intensiva (English Edition)* 37 (4) (2013) 292-298.
- [18] R.S. Campbell B.R. Davis Pressure-controlled versus volume-controlled ventilation: does it matter? *Respiratory care* 47 4 2002 416 424 discussion 424-6.
- [19] Lujan AE, Larsen EW, Balter JM, et al. A method for incorporating organ due to breathing into 3D dose calculations[J]. *Medical Physics*, 1999, 26(5) , 715-720.
- [20] Liu G H, Xiao H J, Yu L H. Simulation Research on Respiratory Power Process under the



Mechanical Properties of Human Respiratory System. Science Technology and Engineering, 2017, 17(29): 313-318.

- [21] Deniz Inal-Ince, Aslihan Cakmak. Chapter 19 - Kinesiology of respiration. Comparative Kinesiology of the Human Body, 2020: 353-363.